1 The formation of nitro-aromatic compounds under high NOx-
2 anthropogenic VOCs dominated atmosphere in summer in Beijing,
3 China

4 Yujue Wang[1], Min Hu[*,1,5], Yuchen Wang[3], Jing Zheng[1], Dongjie Shang[1], Yudong Yang[1], Ying Liu[1,5],
5 Xiao Li[1], Rongzhi Tang[1], Wenfei Zhu[6], Zhuofei Du[1], Yusheng Wu[1], Song Guo[1], Zhijun Wu[1], Shengrong
6 Lou[6], Mattias Hallquist[2], and Jian Zhen Yu [*,3,4]

7 [1]State Key Joint Laboratory of Environmental Simulation and Pollution Control, College of Environmental Sciences and
8 Engineering, Peking University, Beijing 100871, China
9 [2]Department of Chemistry and Molecular Biology, University of Gothenburg, Gothenburg, Sweden
10 [3]Environmental Science Programs, Hong Kong University of Science & Technology, Hong Kong, China
11 [4]Department of Chemistry, Hong Kong University of Science & Technology, Hong Kong, China
12 [5]Beijing Innovation Center for Engineering Sciences and Advanced Technology, Peking University, Beijing 100871, China
13 [6]Shanghai Academy of Environmental Sciences, Shanghai 200233, China

14 *Correspondence to*: Min Hu (minhu@pku.edu.cn); Jian Zhen Yu (jian.yu@ust.hk)

16 **Abstract.** Nitro-aromatic compounds (NACs), as important contributors to ultraviolet light absorption by brown carbon,

17 have been widely observed in various ambient atmospheres, however, few field studies has been focused on their formation

18 in urban atmospheres. In this work, NACs in Beijing were comprehensively quantified and characterized in summer, along

19 with major components in fine particulate matter and selected volatile organic compounds. Field observations in this high

20 NOx-anthropogenic VOCs dominated urban atmosphere were analyzed to investigate the NAC formation and influence

21 factors. The total concentration of quantified NACs was 6.63 ng/m^3, higher than other summertime studies (0.14- 6.44

22 ng/m^3). 4-Nitrophenol (4NP, 32.4%) and 4-nitrocatechol (4NC, 28.5%) were the most abundant ones among all the

23 quantified NAC species, followed by methyl-nitrocatechol (MNC), methyl-nitrophenol (MNP) and dimethyl-nitrophenol

24 (DMNP). The oxidation of toluene and benzene in the presence of NOx were found to be more dominant sources of NACs

25 than biomass burning emissions. The NO$_2$ level was an important factor influencing the secondary formation of NACs. A

26 transition from low- to high-NOx regimes coincided with a shift from organic- to inorganic-dominated oxidation products.

27 The transition thresholds were NO$_2$~20 ppb for daytime and NO$_2$~25 ppb for nighttime conditions. Under low-NOx

28 conditions, NACs increased with NO$_2$, while the NO$_3^-$ concentrations and (NO$_3^-$)/NACs ratios were lower, implying

29 organic-dominated products. Above the NOx regime transition values, NO$_2$ was excess for the oxidation of ambient VOCs.

30 Under this condition, NAC concentrations did not further increase obviously with NO$_2$, while the NO$_3^-$ concentrations and

31 (NO$_3^-$)/NACs ratios showed significant increasing trends, when shifting from organic- to inorganic-dominated products.

32 Obvious nighttime enhancements of 3M4NC and 4M5NC, daytime enhancements of 4NP, 2M4NP and DMNP indicated

33 their different formation pathways. The aqueous-phase oxidation was the major formation pathways of 4M5NC and 3M5NC,

34   and photo-oxidation of toluene and benzene in the presence of NO_2 could be more important for the formation of nitrophenol

35   and its derivatives. Thus, the (3M4NC+ 4M5NC)/4NP ratios was employed to indicate the relative contribution of

36   aqueous-phase and gas-phase oxidation to NAC formation. The relative contribution of aqueous-phase pathways was

37   observed to increase at elevated ambient RH and remain constant at RH> 30%. In addition, the concentrations of VOC

38   precursors (e.g. toluene and benzene) and aerosol surface area were also important factors promoting NAC formation, and

39   photolysis was an important loss pathway of NACs.

40

1   Introduction

42   Organic nitrogen, including nitro-aromatic compounds (NACs), N-heterocyclic compounds, amines and other organic

43   nitrate compounds containing $(-NO_2)$ or $(-NO_3)$ functional groups, represent an important fraction of ambient organic

44   aerosols (Laskin et al., 2009; Wang et al., 2017b; Chow et al., 2016; Ge et al., 2011; Ng et al., 2017). Among organic

45   nitrogen, NACs, with the $-NO_2$ and $-OH$ functional groups attached to an aromatic ring, have gained much attention due to

46   their impacts on light-absorption and human health (Mohr et al., 2013; Lin et al., 2017). NACs, including nitrophenols (NPs),

47   nitrocatechols (NCs) and their derivatives, are important contributors to ultraviolet light absorption by brown carbon (BrC)

48   (Mohr et al., 2013; Teich et al., 2017; Zhang et al., 2013; Xie et al., 2017), contributing 50-80% of the total visible light

49   absorption by BrC emitted from biomass burning (Lin et al., 2017). Moreover, NACs also lead to mutagenesis and

50   genotoxicity, thus posing a threat to human health (Purohit and Basu, 2000; Huang et al., 1995).

51   NACs have been widely observed in various ambient atmospheres, including urban, suburban, rural, as well as

52   background environments, with the quantified concentrations varying from 0.1 ng/m^3 in rural background area to 147.4

53   ng/m^3 in urban area (Iinuma et al., 2010; Teich et al., 2017; Zhang et al., 2010; Mohr et al., 2013; Chow et al., 2016; Wang et

54   al., 2018b). Combustion processes, especially biomass burning, were one of the most important primary sources of NACs

55   (Harrison et al., 2005; Wang et al., 2018b). The emission factors of NACs from biomass burning were estimated 0.8-11.1

56   mg/kg (Wang et al., 2017a; Hoffmann et al., 2007). Field observation studies indicated NACs are usually associated with

57   fresh or aged biomass burning aerosols, which contributed 10- 21% of the total NACs in ambient aerosols (Chow et al., 2016;

58   Kitanovski et al., 2012; Mohr et al., 2013; Iinuma et al., 2010; Wang et al., 2018b). Apart from direct emissions from

59   biomass burning, NACs could also form through the oxidation of volatile organic compounds (VOCs, e.g. cresol, catechol)

60   emitted from biomass burning in the smoke plumes (Iinuma et al., 2010; Claeys et al., 2012). Methyl-nitrocatechols (MNCs)

61   could originate from NO_x oxidation of cresol or catechol, which are released during biomass burning as thermal degradation

62   products of lignin (Iinuma et al., 2010; Finewax et al., 2018; Olariu et al., 2002).

63   Various gas-phase and condensed-phase oxidation of anthropogenic VOC precursors are also important contributors to

64   NAC formation, especially in urban atmospheres (Harrison et al., 2005). The main reactions leading to the secondary

65 formation of NPs, NCs, methyl-nitrophenols (MNPs) and MNCs are shown in Figure 1 (Jenkin et al., 2003). Nitrophenols

66 and its derivatives (e.g. MNPs) could originate through gas-phase oxidation of aromatic hydrocarbons (e.g. phenol, benzene

67 and toluene) by OH or NO_3 radicals in the presence of NO_2, which could represent the major sources of NPs in some

68 environments (Harrison et al., 2005; Yuan et al., 2016; Sato et al., 2007; Ji et al., 2017; Olariu et al., 2002). Nitrocatechols

69 dominated the composition of NACs formed in benzene/NO_x system (Xie et al., 2017). The NC formation could be initiated

70 by OH or NO_3 radicals to form β-hydroxyphenoxy/o-semiquinone radicals, which then react with NO_2 to form the final

71 products (Finewax et al., 2018). Compared with the gas-phase formation of NACs, the NAC formation via aqueous-phase

72 aromatic nitration is less well understood. Nitrophenols could form through the nitration and hydroxylation of benzene in the

73 presence of nitrite/nitrous acid or photo-nitration of phenol upon UV irradiation of nitrite in aqueous solutions (Vione et al.,

74 2004; Vione et al., 2001). It has been suggested that nighttime aqueous-phase oxidation is an important formation pathway

75 for methyl-nitrocatechols, especially in polluted high-NO_x environments and acidic particles (pH around 3) (Vidovic et al.,

76 2018). The proposed aqueous-phase formation processes of MNCs include electrophilic substitution route and consecutive

77 oxidation and conjugated addition route (Frka et al., 2016; Vidovic et al., 2018). The proposed loss pathways for NACs

78 include photolysis and reactions with OH, NO_3 radicals or chlorine atoms (Atkinson et al., 1992; Bejan et al., 2007; Bejan et

79 al., 2015; Chen et al., 2011; Yuan et al., 2016).

80   However, few studies have been conducted based on field observation to investigate the formation of NACs in urban

81 atmospheres. To get a comprehensive understanding on the characteristics and sources of NACs in high NO_x-anthropogenic

82 VOCs dominated atmospheres, an intensive field campaign was conducted in Beijing. A group of NACs (NPs, MNPs,

83 dimethyl-nitrophenols, DMNPs, NCs and MNCs) were comprehensively quantified and characterized using high

84 performance liquid chromatography- mass spectrometry (HPLC-MS). Focusing on the secondary formation of NACs,

85 previous lab study results were applied to the ambient atmosphere in urban Beijing and the influence factors of NAC

86 formation were comprehensively analyzed. This work illustrates the secondary formation of NACs in high

87 NO_x-anthropogenic VOCs dominated urban environments.

88 **2   Methods**

89 **2.1 Sample collection**

90   Within the bilateral Sweden-China framework research program on 'Photochemical smog in China', an intensive field

91 campaign was conducted in Beijing to improve the understanding on secondary chemistry during photochemical smog in

92 China (Hallquist et al., 2016). The campaign was conducted at Changping (40.14° N, 116.11° E), a regional site northeast of

93 Beijing urban area, from May 15 to June 5, 2016, when the site was obviously influenced by anthropogenic pollutants from

94 Beijing urban areas and under high-NO_x conditions (Tang et al., 2018; Wang et al., 2018a). During May 17- June 5, the daily

95 average concentrations of benzene, toluene and NO_x were 66-922 ppt, 47-1344 ppt and 4.0-32.3 ppb, respectively.

96   Ambient $PM_{2.5}$ (particles with aerodynamic diameter less than 2.5 μm) samples were collected on prebaked quartz fiber

97 filters (Whatman Inc.) and Teflon filters (Whatman Inc.) using a high-volume sampler (TH-1000C, Tianhong, China) and a

98 4-channel sampler (TH-16A, Tianhong, China) during the campaign. The sampling flow rates were 1.05 m^3/min and 16.7

99 L/min, respectively. The daytime samples were collected from 8:30 to 17:30 LT (UTC+8) and nighttime ones from 18:00 to

100 8:00 LT (UTC+8) the next morning. Field blank samples were collected by placing filters in the samplers with the pump off

101 for 30 min.

102 **2.2 Quantification of NACs**

103   An aliquot of 25 cm^2 was removed from each filter sample and extracted in ultrasonic bath three times using 3, 2 and 1

104 mL methanol containing 30 μL saturated EDTA solution in methanol-acetic acid consecutively, each time for 30 min. The

105 extracts were then filtered through a 0.25 μm polytetrafluoroethylene (PTFE) syringe filter (Pall Life Sciences), combined,

106 and evaporated to dryness under a gentle stream of high-purity nitrogen. The dried samples were re-dissolved in 50 μL

107 methanol/water (1:1) containing 100 ppb 4-nitrophenol-2,3,5,6-d_4 as internal standard. The solution was centrifuged and the

108 supernatant was used for analysis, using Agilent 1260 LC system (Palo Alto, CA) coupled to QTRAP 4500 (AB Sciex,

109 Toronto, Ontario, Canada) mass spectrometer. The LC-MS system was equipped with an electrospray ionization (ESI)

110 source operated in negative mode. More details of the extraction and optimized MS parameters have been described in our

111 previous study (Chow et al., 2016).

112   Chromatographic separation was performed on an Acquity UPLC HSS T3 column (2.1 mm×100 mm, 1.8 μm particle

113 size; Waters, USA) with a guard column (HSS T3, 1.8 μm). The column temperature was kept at 45 $^\circ$C and the injection

114 volume was 5.0 μL. The mobile eluents were (A) water containing 0.1% acetic acid (v/v) and (B) methanol (v/v) containing

115 0.1% acetic acid at a flow rate of 0.19 mL/min. The gradient elution was set as follows: started with 1% B for 2.7 min;

116 increased to 54% B within 12.5 min and held for 1.0 min; then increased to 90% B within 7.5 min and held for 0.2 min; and

117 finally decreased to 1% B within 1.8 min and held for 17.3 min until the column was equilibrated.

118   The quantified NAC species are listed in Table 1. The NACs were identified and quantified using the [M-H]$^-$ ions in the

119 extracted ion chromatogram (EIC), using authentic standards or surrogates with the same molecular formula (Table 1). The

120 standards included: 4-nitrocatechol (4NC), 4-nitrophenol (4NP), 2-methyl-4-nitrophenol (2M4NP), 3-methyl-4-nitrophenol

121 (3M4NP) and 2,6-dimethyl-4-nitrophenol (2,6DM4NP) from Sigma–Aldrich (St. Louis, MO, USA);

122 4-methyl-5-nitrocatechol (4M5NC) from Santa Cruz Biotech (Dallas, TX, USA). The concentration of dimethyl-nitrophenol

123 (DMNP) was the sum of three isomers.

2.3 Other online and offline measurements

124

125   Other online and offline instruments were also employed to obtain related database, which has been introduced in detail

126   in our previous paper (Wang et al., 2018c). A high resolution time-of-flight aerosol mass spectrometer (AMS) was used to

127   measure the chemical composition of PM_1 (Zheng et al., 2017). The aerosol surface area was calculated based on the

128   measurements of particle number and size distribution by a scanning mobility particle sizer (SMPS, TSI 3936) and an

129   aerosol particle sizer (APS, TSI 3321) (Yue et al., 2009; Wang et al., 2018a). VOCs were measured by a

130   proton-transfer-reaction mass spectrometer (PTR-MS). Gaseous NH_3 was measured using a NH_3 analyzer (G2103, Picarro,

131   California, USA) (Huo et al., 2015). Meteorological parameters, including relative humidity (RH), temperature, wind

132   direction and wind speed (WS) were continuously monitored by a weather station (Met one Instrument Inc.) during the

133   whole campaign.

134   Organic carbon (OC) was analyzed using thermal/optical carbon analyzer (Sunset Laboratory). The organic matter (OM)

135   concentration was calculated by multiplying OC by 1.6 (Turpin and Lim, 2001). Water soluble inorganic ions were

136   quantified by an ion chromatograph (IC, DIONEX, ICS2500/ICS2000) following procedures described in Guo et al. (2010).

137   Aerosol acidity was then calculated using the ISORROPIA-II thermodynamic model. ISORROPIA-II was operated in

138   forward mode, assuming the particles are "metastable" (Hennigan et al., 2015; Weber et al., 2016; Guo et al., 2015). The

139   input parameters included: ambient RH, temperature, particle phase inorganic species (SO_4^{2-}, NO_3^-, Cl^-, NH_4^+, K^+, Na^+, Ca^{2+},

140   Mg^{2+}), and gaseous NH_3. More details and validation of the thermodynamic calculations have been described in our previous

141   paper (Wang et al., 2018c).

3   Results and discussion

142

143   **3.1 Concentration and composition of NACs**

144   The average concentration of quantified NACs was 6.63 ng/m^3, ranging from 1.27 to 17.70 ng/m^3 in summer in Beijing.

145   The concentrations of total NACs as well as individual species across this and prior studies were summarized and compared

146   in Figures 2, S1 and Table S1. The total NAC concentration was higher than other studies conducted in summer in mountain,

147   rural or urban environments (Teich et al., 2017; Kitanovski et al., 2012; Kahnt et al., 2013; Zhang et al., 2013; Chow et al.,

148   2016; Wang et al., 2018b), and comparable to the studies in summertime Wangdu, China (Teich et al., 2017; Wang et al.,

149   2018b) (Figure 2). Each NAC species (NP, NC, MNP and MNC), except DMNP, also showed elevated concentrations in

150   Changping, compared with those reported in other summertime studies (Figure S1). Influenced by the outflow from urban

151   Beijing air masses, the site was under typical high-NO_x conditions (Wang et al., 2018a), implying abundant potential

152   secondary formation of NACs during the observation period. A recent study suggested that nocturnal biogenic VOCs

153   (BVOCs) oxidation would transfer from low- to high-NO_x regimes and nearly all the BVOCs would be oxidized by NO_3

154   radicals, at a NO_x/BVOCs ratio higher than 1.4 (Edwards et al., 2017). When we roughly estimated the BVOCs

155   concentration to be the sum of isoprene, MVK+MACR (methyl vinyl ketone and methacrolein), and monoterpenes, the

156   NO_x/BVOC ratios were higher than 8 (nighttime ratios higher than 20) (Figure S2). Even considering the major

157   anthropogenic VOCs (toluene, benzene), NO_x/VOCs ratios were higher than 5 (nighttime ratios higher than 10) (Figure S2).

158   The high-NO_x conditions were expected to facilitate the oxidation of aromatic hydrocarbons and the secondary formation of

159   NACs during the campaign. Other emissions from biomass burning and coal combustion were also observed to be

160   contributors of organic aerosols during the campaign (Tang et al., 2018), which could also be the sources of NACs. Biomass

161   burning episodes occurred during Wangdu campaign, indicating obvious NAC emissions from biomass burning (Teich et al.,

162   2017; Tham et al., 2016), which explain the high NAC levels in summer in Wangdu. The NAC concentrations during

163   summer (including this study) are generally lower than those during spring, autumn or winter, when usually with higher

164   combustion emissions, especially biomass burning and coal combustion (Chow et al., 2016; Wang et al., 2018b; Kitanovski

165   et al., 2012; Kahnt et al., 2013).

166   The NAC compositions are shown in the inserted pie chart in Figure S1. 4-Nitrophenol and 4-nitrocatechol were the

167   most abundant ones among all the quantified NAC species, accounting for 32.4 % and 28.5 % of the total quantified NACs,

168   followed by methyl-nitrocatechol (4M5NC, 3M5NC and 3M6NC, 16.2%), methyl-nitrophenol (2M4NP and 3M4NP, 15.6%)

169   and dimethyl-nitrophenol (8.3%) (Table 1). Nitrophenols and nitrocatechols were generally reported among the most

170   abundant NAC species in previous studies (Table S1 and the references therein). Nitrophenols could form via the oxidation

171   of anthropogenic VOCs (e.g. benzene) in the presence of NO_2 and nitrocatechols dominate the composition of NACs formed

172   in benzene/NO_x system (Xie et al., 2017; Harrison et al., 2005; Yuan et al., 2016; Sato et al., 2007; Ji et al., 2017; Olariu et

173   al., 2002). Thus, the high contributions of nitrophenol and nitrocatechol were not surprising in the typical high

174   NO_x-anthropogenic VOCs dominated environments in summer in Beijing.

175   The contribution of NP among the total NACs at Changping was higher than that in summer in Hong Kong, while that

176   of MNC was lower (Table S1 and the inserted pie charts in Figure S1). The gas-phase oxidation of aromatic hydrocarbons

177   (e.g. phenol, benzene) in the presence of NO_2 is a major source of NPs (Harrison et al., 2005; Yuan et al., 2016; Sato et al.,

178   2007; Ji et al., 2017; Olariu et al., 2002), while aqueous-phase oxidation represents the important formation pathway for

179   atmospheric MNC (Frka et al., 2016; Vidovic et al., 2018). Different NAC compositions between Changping and Hong

180   Kong potentially hint difference in the relative contribution of aqueous-phase and gas-phase pathways to NAC formation

181   under different environment conditions. The ambient RH in Hong Kong was obviously higher than that in summer in Beijing

182   (Zhao et al., 2016), thus the relative contribution of aqueous-phase pathways could be more dominant, promoting the

183   aqueous-phase formation of MNC in Hong Kong. The influence of ambient RH on NAC formation would be further

184   discussed in section 4.2. More abundant gas-phase formation of nitrophenol was expected in summer in Beijing, under

185   higher anthropogenic VOCs, high NO_x and low RH conditions. What's more, the temperature in summer in Changping was

186   lower than that in summer in Hong Kong (Zhao et al., 2016), which was more favorable for the partitioning of nitrophenol

187   products from gas phase into particle phase.

3.2 Temporal variation and sources of NACs

189   Temporal variations of the total quantified NAC concentrations in this study are shown in Figure 3, along with

190   particulate organics, nitrate, potassium ion, toluene, benzene, wind speed and RH. The correlation analysis between NACs

191   and other chemical components or meteorological conditions is shown in Table S2. During the observation period, four

192   pollution episodes (episodes I, II, III, IV) were identified based on the organic aerosols, marked by gray shading in Figure 3.

193   Elevated NAC concentrations were observed during each pollution episode, coincided with the increasing of toluene,

194   benzene and potassium. Their good inter-correlations (Table S2) suggested the sources of NACs from biomass burning

195   emissions and secondary oxidation of anthropogenic VOCs (benzene, toluene and their oxidation products). It was noticed

196   that NACs showed stronger correlations with toluene (r=0.70) or benzene (r=0.64) than those with potassium (r=0.49),

197   indicating the NO_x oxidation of anthropogenic VOCs as more dominant sources of NACs than biomass burning in summer

198   in Beijing.

199   To further investigate the secondary formation of NACs, the time series and day-night variations of individual NAC

200   species are shown in Figures 4, S3 and S4. Obvious daytime enhancements of 4NP, 2M4NP and DMNP, nighttime

201   enhancements of 3M4NC and 4M5NC were observed, and other NAC species didn't show obvious day-night variations

202   (Figures 4, S3 and S4), indicating different formation pathways for NAC species. Good inter-correlations were observed

203   among nitrophenol and its derivatives (2M4NP, 3M4NP, DMNP, r=0.56-0.88), as well as among nitrocatechol and its

204   derivatives (3M6NC, 3M5NC, 4M5NC, r=0.49-0.84). However, the correlations between nitrophenol derivatives and

205   nitrocatechol derivatives (r=0.05-0.45) were lower (Table S2). The correlation analysis indicated that the formation and loss

206   pathways as well as the influence factors were similar within each group (NP and NP derivatives, NC and NC derivatives),

207   while different between them. NC and its derivatives showed stronger correlations with toluene, benzene and K^+, compared

208   with NP and its derivatives (Table S2). This was because the factors influencing the particulate NP distribution could be

209   more complicated. Gas-phase oxidation represents an important formation pathway for NP, thus the distributions of

210   particulate NP could largely dependent on gas-particle partitioning or their gas-phase loss pathways (e.g. photolysis).

211   Obvious nighttime enhancements of 4M5NC and 3M5NC were observed during the whole observation period,

212   especially during the first pollution episode (Figure 4). Strong inter-correlations between 4M5NC and 3M5NC and their

213   similar temporal variations indicated the similar formation pathways. It has been suggested that aqueous-phase oxidation

214   (including photooxidation and nighttime oxidation) is an important formation pathway for atmospheric MNC, especially in

215   polluted high-NO_x environments and relatively acidic particles (pH around 3) (Vidovic et al., 2018; Frka et al., 2016).

216   4M5NC and 3M5NC showed relatively stronger correlations with RH compared with other NAC species (Table S2),

217   implying the importance of water in their formation processes and the aqueous-phase pathway. During the campaign,

218   particles were generally acidic with a pH range of 2.0- 3.7 and under high-NO_x conditions (Wang et al., 2018c; Wang et al.,

219   2018a), which were suitable environments for the aqueous-phase oxidation formation of MNC. The daytime correlations

220   between 4M5NC or 3M5NC and RH or NO_2 were stronger than the nighttime (Table S3). The aqueous-phase NO_x oxidation

221   could be more dependent on ambient RH and NO_2 levels during the daytime, due to the lower RH and NO_2 concentrations

222   than those at night (Figures 3, S2). MNC also showed good correlations with potassium, as MNC could also form via the

223   oxidation of VOC precursors (e.g. cresol, catechol) emitted from biomass burning (Iinuma et al., 2010; Finewax et al., 2018;

224   Olariu et al., 2002). 3M6NC showed different temporal variations from 4M5NC or 3M5NC (Figures 4, S3) and their

225   correlations were lower than that between 4M5NC and 3M5NC (Tables S2, S3), which suggested different formation

226   pathway of 3M6NC from those of 4M5NC or 3M5NC. The quantum calculations have predicted the formation of 3M5NC

227   via aqueous-phase electrophilic substitution and nitration by NO_2^+, while the formation of 3M6NC was negligible due to

228   higher activation barriers for nitration of 3-methylcatechol to form 3M6NC (Frka et al., 2016). A dominant presence of

229   3M5NC in ambient aerosols was also expected according to the theoretical predictions (Frka et al., 2016). The 3M5NC

230   concentration was obviously higher than that of 3M6NC in summer in Beijing, which is consistent with the study in Frka et

231   al. (2016).

232   Different from the nighttime enhancements of 4M5NC and 3M5NC, 4NP, 2M4NP and DMNP showed obvious daytime

233   enhancements during the whole campaign (Figures 4, S4), indicating the importance of photochemical oxidation for the

234   formation of NP and its derivatives. Previous study also suggested the daytime gas-phase oxidation of aromatics could

235   represent the major source of nitrophenols, while the contribution from nighttime reaction of phenol with NO_3 radicals was

236   relatively lower (Yuan et al., 2016). We did not find obvious correlation between 4NP and NO_2 when considering the whole

237   period (Table S2), while good correlations were observed when treating the daytime and nighttime conditions separately

238   (Table S3). The strong correlations between 4NP and benzene, toluene or NO_2 during daytime and nighttime indicated its

239   formation via oxidation of benzene and toluene in the presence of NO_2 (Table S3). The formation mechanisms of nitrophenol

240   were different during daytime (OH-initiated photooxidation of aromatics in the presence of NO_2) and nighttime

241   (NO_3-initiated oxidation of aromatics) (Harrison et al., 2005; Yuan et al., 2016; Sato et al., 2007; Ji et al., 2017; Olariu et al.,

242   2002), thus the role and influence of NO_2 on NAC formation were different. For DMNP, 2M4NP and 3M4NP, they also

243   showed good correlations with benzene, toluene and NO_2 during daytime, which indicated their potential formation

244   pathways via photooxidation of aromatics in the presence of NO_2. However, DMNP and 3M4NP didn't show correlations

245   with benzene, toluene or NO_2 at night. Their correlations with RH were higher at night, implying the possible formation

246   related to aqueous-phase pathways, while the potential precursors or mechanisms remain unknown.

247

4   Discussion

4.1 The NO$_2$ control of NACs formation

NO$_x$ oxidation of anthropogenic VOC precursors represented the dominant sources of NACs in summer in Beijing. To further investigate the impacts of NO$_2$ on NAC secondary formation, we plot the concentrations of NACs, nitrate (NO$_3^-$) and the NO$_3^-$/NAC ratios as a function of NO$_2$ levels (Figure 5). The variation of (NO$_3^-$)/NACs ratios was employed to illustrate the relative abundance of inorganic nitrate and oxidized organic nitrogen. The variation during daytime and nighttime were separately considered due to the different atmospheric conditions and oxidation mechanisms (Figure 1).

Generally, higher concentrations of NACs and nitrate were observed with elevated NO$_2$ concentration levels, with nonlinear responses (Figure 5). During the daytime, the NACs increased with NO$_2$, and the NO$_3^-$ concentrations and (NO$_3^-$)/NACs ratios were lower at low-NO$_x$ conditions (NO$_2$< 20ppb). As NO$_2$ increased to higher than 20 ppb, the NAC concentration did not obviously increase with NO$_2$ any more, indicating the transition from NO$_x$-sensitive to NO$_x$-saturated regimes for NAC secondary formation. At the same time, the NO$_3^-$ concentrations and (NO$_3^-$)/NACs ratios showed significant increasing trends (Figure 5a, b, c). It was likely that the daytime NO$_2$ was excess for the oxidation of ambient VOCs and the NAC formation at NO$_2$> 20 ppb. The excess NO$_2$ would be oxidized to form inorganic nitrate, indicating the shift of products from organic- to inorganic-dominated conditions. Similarly, the transitions from the low- to high-NO$_x$ regimes and oxidation products from organic- to inorganic-dominated were also observed at NO$_2$ ~25 ppb at night under the ambient environments in summer in Beijing (Figure 5d, e, f). The nighttime NAC formation would become independent of NO$_2$ concentrations and inorganic nitrate dominated the NO$_x$ oxidation products at NO$_2$> 25 ppb. The simplified mechanisms and schematic diagram of the competing formation of inorganic nitrates and NACs are shown in Figure S5. The nighttime NO$_2$ transition value (~25 ppb) was higher than the daytime one (~20 ppb). The higher anthropogenic VOC precursors (Figure S2) and different oxidation mechanisms at night (Figure 1) were the potential reasons for elevated NO$_2$ transition value.

Taking NACs as an example, the result implied that the transition from low- to high-NO$_x$ regimes and the oxidation products shifting from organic- to inorganic-dominated conditions existed in the anthropogenic VOCs-NO$_x$ interacted conditions in polluted urban atmospheres. However, the mechanisms as well as transition thresholds were less understood compared with the well-known BVOCs-NO$_x$ interaction atmospheres. The NO$_x$ transition regimes of more organic nitrogen formation and the oxidation mechanisms during daytime and nighttime deserve comprehensive investigation in anthropogenic VOCs-NO$_x$ interacted urban atmospheres. Due to the complex VOC composition in ambient atmosphere and the limited number of VOC species measured in this study, the NO$_x$ regime transition value was expressed by NO$_2$ concentrations under the condition of urban Beijing atmospheres rather than NO$_2$/VOC or NO$_x$/VOC ratios. The NO$_x$ regime transition values deserve further investigation based on comprehensive lab simulation and field observations, which could be

279   expressed by NO_x/VOC ratios and applied to various atmospheric environments.

280   The formation pathways of different NAC species vary from each other based on the analysis in sections 3.2, thus the

281   role and influence of NO_2 on their formation are different. The variation of NAC compositions as a function of NO_2 levels is

282   shown in Figure 6 to investigate the influence of NO_2 on NAC compositions. The contributions of nitrocatechol and its

283   derivatives among the total NACs increased and those of nitrophenol and its derivatives decreased at elevated NO_2

284   concentrations. The NAC composition remained relatively constant at NO_2 >20 ppb, which was approximately the transition

285   value from low- to high-NO_x regimes. The role of elevated NO_2 in promoting NC (and its derivatives) formation was more

286   obvious than that for NP (and its derivatives). The oxidation of aromatics (e.g. benzene, toluene and VOCs emitted from

287   biomass burning) in the presence of NO_2 represent the major formation pathway of NC and its derivatives based on the

288   analysis in section 3.2. The formation of NC and its derivatives would increase obviously as the increasing of ambient NO_2

289   concentration levels. The distributions of nitrophenol and its derivatives could also be obviously influenced by the

290   gas-particle partitioning and their loss pathways (e.g. photolysis), thus their increasing trend as a function of NO_2 was not as

291   obvious as those of NC and its derivatives.

292

4.2 Other influence factors of NACs formation

294   Nitration of aromatic hydrocarbons (e.g. benzene and toluene) represents the major source of NACs in summer in

295   Beijing. NACs generally increased with the increasing of anthropogenic toluene and benzene (Figure 7). During daytime,

296   when toluene was higher than 0.6 ppb and benzene higher than 0.4 ppb, the NACs concentrations would not increase further

297   with VOC concentrations (Figure 7a, b). It was likely that toluene or benzene was in excess and the NAC formation became

298   independent of anthropogenic VOC precursors under this condition. Similarly, the nighttime formation of NACs would be

299   independent of anthropogenic VOCs, when toluene was higher than 1 ppb and benzene higher than 0.6 ppb (Figure 7c, d).

300   The transition values of toluene or benzene was higher at night than those during the daytime. This could be due to the

301   significantly higher NO_2 levels (Figure S2), with higher capacity to oxidize VOC precursors, and different oxidation

302   mechanisms at night.

303   Though the total NACs didn't show good correlations with ambient RH, good correlations between 3M4NC, 4M5NC

304   and RH were observed (Table S2, Figure 8). The NAC products (e.g. nitrophenols) dominated by gas-phase formation

305   pathways were less affected by ambient RH. Aqueous-phase oxidation represented the major formation pathway of 3M4NC

306   and 4M5NC during the campaign, based on the analysis in section 3.2 and previous studies (Vidovic et al., 2018; Frka et al.,

307   2016). Elevated ambient RH would favor the water uptake of aerosols and decrease the aerosol viscosity, which favors the

308   exchange of organic precursors or other gas molecules into the particles, mass diffusion of reactants and chemical reactions

309   within the particles (Vaden et al., 2011; Booth et al., 2014; Renbaum-Wolff et al., 2013; Shrestha et al., 2015; Zhang et al.,

310   2015), and thereby enhance the formation of 3M4NC and 4M5NC in aqueous phase. The (3M4NC+ 4M5NC)/4NP mass

311   concentration ratios were employed to indicate the relative contribution of aqueous-phase and gas-phase pathways to NAC

312   formation. The variations of (3M4NC+ 4M5NC)/4NP ratios as a function of ambient RH during daytime and nighttime were

313   shown in Figure 9. The (3M4NC+ 4M5NC)/4NP ratios increased under higher RH conditions during the daytime, indicating

314   elevated contribution of aqueous-phase pathways to NAC formation. The relative contribution of aqueous-phase and

315   gas-phase pathways would not increase further as the increasing of RH at RH > 30%, indicated by the stable (3M4NC+

316   4M5NC)/4NP ratios (Figure 9a). The relative contribution of aqueous-phase and gas-phase pathways remained constant

317   under higher RH conditions (RH> 30%) at night (Figure 9b). The nighttime (3M4NC+ 4M5NC)/4NP ratios were obviously

318   higher than the daytime ones, which implied that the aqueous-phase oxidation played more important roles for NAC

319   formation at night. The results implied the importance of aqueous-phase oxidation for the secondary formation of oxidized

320   organic nitrogen at elevated ambient RH. Due to the limited sample number obtained by filter-based analysis in this study,

321   the influence of RH or aerosol liquid water content on NAC formation needs further investigation using online

322   measurements in the lab.

323   The NAC concentrations also showed good correlations with aerosol surface area (Figure 8b). Higher aerosol surface

324   area would provide a good interface for the partitioning of gas-phase NAC products into particle phase and also for the

325   aqueous-phase or heterogeneous oxidation processes to form NACs (Frka et al., 2016; Vidovic et al., 2018; Bauer et al., 2004;

326   Fenter et al., 1996). Photolysis is an important loss pathway of NACs and could be the dominant sink for nitrophenol in the

327   gas phase (Bejan et al., 2007; Yuan et al., 2016). The highest value of $J(O^1D)$ of each day was used to roughly represent the

328   photolysis intensity. The daytime NAC concentrations showed negative correlations with $J(O^1D)$ (Figure 8c, Table S3),

329   suggesting photolysis as an important sink for NACs during the daytime.

330

331   **5   Conclusions**

332   Nitroaromatic compounds (NACs), as important contributors to ultraviolet light absorption by brown carbon, have been

333   widely observed in various ambient atmospheres. An intensive field campaign was conducted in summer in Beijing, to

334   investigate the characterization and formation of NACs under high NO_x-anthropogenic VOCs dominated atmosphere. NACs

335   were comprehensively quantified and characterized using HPLC-MS. The total concentration of quantified NACs was 6.63

336   ng/m³, ranging from 1.27 to 17.70 ng/m³, generally higher than those reported in other studies conducted in summer.

337   4-Nitrophenol (32.4%) and 4-nitrocatechol (28.5%) were the most abundant NAC species, consistent with previous studies,

338   and followed by methyl-nitrocatechol, methyl-nitrophenol and dimethyl-nitrophenol.

339   The oxidation of anthropogenic VOC precursors (e.g. toluene, benzene and their oxidation products) in the presence of

340   NO_2 represented more important sources of NACs than biomass burning in summer in Beijing. NO_2 plays important roles in

341   the secondary formation of NACs. A transition from low- to high-NO_x regimes and oxidation products from organic- to

342   inorganic-dominated conditions were observed, which was $NO_2 \sim 20$ ppb for the daytime and $NO_2 \sim 25$ ppb for the nighttime

343   atmosphere. Under low-NO_x conditions, NACs were observed to increase with NO_2, and the NO_3^- concentrations and

344   (NO_3^-)/NACs ratios were lower. As NO_2 increased to the high-NO_x regimes, the NAC concentration did not further increase

345   obviously with NO_2, and the NO_3^- concentrations and (NO_3^-)/NACs ratios would show obvious increasing trends. Using

346   NACs as an example of organic nitrogen, the low- and high-NO_x regimes were observed in the anthropogenic VOCs-NO_x

347   interacted conditions in polluted urban atmospheres. While the mechanisms as well as transition threshold are still unclear,

348   which deserves comprehensive investigation in future studies.

349   Obvious nighttime enhancements of 3M4NC and 4M5NC, daytime enhancements of 4NP, 2M4NP and DMNP were

350   observed, indicating their different formation pathways. The aqueous-phase oxidation pathways are presumed to be

351   important for the formation of 4M5NC and 3M5NC, under the conditions of polluted high-NO_x and acidic particles during

352   the campaign. Photo-oxidation of toluene and benzene in the presence of NO_2 were more important for the formation of

353   nitrophenol and its derivatives. To further investigate the NAC formation pathways and influence of RH, the (3M4NC+

354   4M5NC)/4NP mass ratios was employed to represent the relative contribution of aqueous-phase and gas-phase pathways to

355   NAC formation. The (3M4NC+ 4M5NC)/4NP mass ratios would increase at elevated RH and remain relatively consistent at

356   RH> 30%, indicating elevated contribution of aqueous-phase pathways to NAC formation under higher RH conditions.

357   Aqueous-phase oxidation played more important roles in NAC formation at night than that during the daytime.

358   VOC precursors, aerosol surface area and photolysis were also important factors influencing the NAC formation.

359   Nitration of aromatic hydrocarbons (e.g. benzene and toluene) represents the major secondary source of NACs, thus NACs

360   generally increased with the increasing of toluene and benzene. The NAC formation would become independent of toluene

361   and benzene, when the daytime concentrations were higher than 0.6 and 0.4 ppb, or the nighttime ones higher than 1 and 0.6

362   ppb. In addition, aerosol surface area was also important factor promoting the NAC formation and photolysis could be an

363   important loss pathway of NACs during the daytime.

364

365

366   *Data availability.* The data presented in this article are available from the authors upon request (minhu@pku.edu.cn).

367

368   **The Supplement related to this article is available online**

369

370   *Author contributions*. MiH, MaH, and SG organized the field campaign. YJW and YCW conducted the offline analysis and

371   analyzed the data. YJW wrote the manuscript with input from JY. All authors contributed to the measurements, discussing

372   results and commenting on the manuscript.

373

374   *Competing interests*. The authors declare that they have no conflict of interest.

375

376   *Acknowledgements*. This work was supported by National Natural Science Foundation of China (91544214, 41421064,

377   51636003); National research program for key issues in air pollution control (DQGG0103); National Key Research and

378   Development Program of China (2016YFC0202000: Task 3); bilateral Sweden-China framework program on

379   'Photochemical smog in China: formation, transformation, impact and abatement strategies' by the Swedish Research

380   council VR under contract (639-2013-6917).

381

382

383

384   **References:**

385   Atkinson, R., Aschmann, S. M., and Arey, J.: Reactions of hydroxyl and nitrogen trioxide radicals with phenol, cresols, and
386   2-nitrophenol at 296 ± 2 K, Environ. Sci. Technol., 26, 1397-1403, 10.1021/es00031a018, 1992.

387   Bauer, S. E., Balkanski, Y., Schulz, M., Hauglustaine, D. A., and Dentener, F.: Global modeling of heterogeneous chemistry
388   on mineral aerosol surfaces: influence on tropospheric ozone chemistry and comparison to observations, J. Geophys. Res.,
389   [Atmos.], 109, 10.1029/2003jd003868, 2004.

390   Bejan, I., Barnes, I., Olariu, R., Zhou, S., Wiesen, P., and Benter, T.: Investigations on the gas-phase photolysis and OH
391   radical kinetics of methyl-2-nitrophenols, Phys. Chem. Chem. Phys., 9, 5686-5692, 10.1039/b709464g, 2007.

392   Bejan, I., Duncianu, M., Olariu, R., Barnes, I., Seakins, P. W., and Wiesen, P.: Kinetic study of the gas-phase reactions of
393   chlorine atoms with 2-chlorophenol, 2-nitrophenol, and four methyl-2-nitrophenol isomers, J. Phys. Chem. A, 119,
394   4735-4745, 10.1021/acs.jpca.5b02392, 2015.

395   Booth, A. M., Murphy, B., Riipinen, I., Percival, C. J., and Topping, D. O.: Connecting bulk viscosity measurements to
396   kinetic limitations on attaining equilibrium for a model aerosol composition, Environ. Sci. Technol., 48, 9298-9305,
397   10.1021/es501705c, 2014.

398   Chen, J., Wenger, J. C., and Venables, D. S.: Near-ultraviolet absorption cross sections of nitrophenols and their potential
399   influence on tropospheric oxidation capacity, J. Phys. Chem. A, 115, 12235-12242, 10.1021/jp206929r, 2011.

400   Chow, K. S., Huang, X. H. H., and Yu, J. Z.: Quantification of nitroaromatic compounds in atmospheric fine particulate
401   matter in Hong Kong over 3 years: field measurement evidence for secondary formation derived from biomass burning
402   emissions, Environ. Chem., 13, 665-673, 10.1071/en15174, 2016.

403   Claeys, M., Vermeylen, R., Yasmeen, F., Gomez-Gonzalez, Y., Chi, X. G., Maenhaut, W., Meszaros, T., and Salma, I.:
404   Chemical characterisation of humic-like substances from urban, rural and tropical biomass burning environments using
405   liquid chromatography with UV/vis photodiode array detection and electrospray ionisation mass spectrometry, Environ.
406   Chem., 9, 273-284, 10.1071/EN11163, 2012.

407   Edwards, P. M., Aikin, K. C., Dube, W. P., Fry, J. L., Gilman, J. B., de Gouw, J. A., Graus, M. G., Hanisco, T. F., Holloway,
408   J., Huber, G., Kaiser, J., Keutsch, F. N., Lerner, B. M., Neuman, J. A., Parrish, D. D., Peischl, J., Pollack, I. B., Ravishankara,
409   A. R., Roberts, J. M., Ryerson, T. B., Trainer, M., Veres, P. R., Wolfe, G. M., Warneke, C., and Brown, S. S.: Transition from

410   high- to low-NO$_x$ control of night-time oxidation in the southeastern US, Nature Geosci., 10, 490-495, 10.1038/NGEO2976,
411   2017.

412   Fenter, F. F., Caloz, F., and Rossi, M. J.: Heterogeneous kinetics of N$_2$O$_5$ uptake on salt, with a systematic study of the role of
413   surface presentation (for N$_2$O$_5$ and HNO$_3$), J. Phys. Chem., 100, 1008-1019, 10.1021/jp9503829, 1996.

414   Finewax, Z., de Gouw, J. A., and Ziemann, P. J.: Identification and quantification of 4-nitrocatechol formed from OH and
415   NO$_3$ radical-initiated reactions of catechol in air in the presence of NO$_x$: implications for secondary organic aerosol
416   formation from biomass burning, Environ. Sci. Technol., 52, 1981-1989, 10.1021/acs.est.7b05864, 2018.

417   Frka, S., Sala, M., Kroflic, A., Hus, M., Cusak, A., and Grgic, I.: Quantum chemical calculations resolved identification of
418   methylnitrocatechols in atmospheric aerosols, Environ. Sci. Technol., 50, 5526-5535, 10.1021/acs.est.6b00823, 2016.

419   Ge, X., Wexler, A. S., and Clegg, S. L.: Atmospheric amines – part I. A review, Atmos. Environ., 45, 524-546,
420   10.1016/j.atmosenv.2010.10.012, 2011.

421   Guo, H., Xu, L., Bougiatioti, A., Cerully, K. M., Capps, S. L., Hite, J. R., Carlton, A. G., Lee, S. H., Bergin, M. H., Ng, N. L.,
422   Nenes, A., and Weber, R. J.: Fine-particle water and pH in the southeastern United States, Atmos. Chem. Phys., 15,
423   5211-5228, 10.5194/acp-15-5211-2015, 2015.

424   Guo, S., Hu, M., Wang, Z. B., Slanina, J., and Zhao, Y. L.: Size-resolved aerosol water-soluble ionic compositions in the
425   summer of Beijing: implication of regional secondary formation, Atmos. Chem. Phys., 10, 947-959,
426   10.5194/acp-10-947-2010, 2010.

427   Hallquist, M., Munthe, J., Hu, M., Wang, T., Chan, C. K., Gao, J., Boman, J., Guo, S., Hallquist, A. M., Mellqvist, J.,
428   Moldanova, J., Pathak, R. K., Pettersson, J. B. C., Pleijel, H., Simpson, D., and Thynell, M.: Photochemical smog in China:
429   scientific challenges and implications for air-quality policies, Natl. Sci. Rev., 3, 401-403, 10.1093/nsr/nww080, 2016.

430   Harrison, M. A. J., Barra, S., Borghesi, D., Vione, D., Arsene, C., and Iulian Olariu, R.: Nitrated phenols in the atmosphere: a
431   review, Atmos. Environ., 39, 231-248, 10.1016/j.atmosenv.2004.09.044, 2005.

432   Hennigan, C. J., Izumi, J., Sullivan, A. P., Weber, R. J., and Nenes, A.: A critical evaluation of proxy methods used to
433   estimate the acidity of atmospheric particles, Atmos. Chem. Phys., 15, 2775-2790, 10.5194/acp-15-2775-2015, 2015.

434   Hoffmann, D., Iinuma, Y., and Herrmann, H.: Development of a method for fast analysis of phenolic molecular markers in
435   biomass burning particles using high performance liquid chromatography/atmospheric pressure chemical ionisation mass
436   spectrometry, J. Chromatogr., A, 1143, 168-175, 10.1016/j.chroma.2007.01.035, 2007.

437   Huang, Q., Wang, L., and Han, S.: The genotoxicity of substituted nitrobenzenes and the quantitative structure-activity
438   relationship studies, Chemosphere, 30, 915-923, 10.1016/0045-6535(94)00450-9, 1995.

439   Huo, Q., Cai, X., Kang, L., Zhang, H., Song, Y., and Zhu, T.: Estimating ammonia emissions from a winter wheat cropland
440   in North China Plain with field experiments and inverse dispersion modeling, Atmos. Environ., 104, 1-10,
441   10.1016/j.atmosenv.2015.01.003, 2015.

442   Iinuma, Y., Boge, O., Grafe, R., and Herrmann, H.: Methyl-nitrocatechols: atmospheric tracer compounds for biomass
443   burning secondary organic aerosols, Environ. Sci. Technol., 44, 8453-8459, 10.1021/es102938a, 2010.

444   Jenkin, M. E., Saunders, S. M., Wagner, V., and Pilling, M. J.: Protocol for the development of the Master Chemical
445   Mechanism, MCM v3 (Part B): tropospheric degradation of aromatic volatile organic compounds, Atmos. Chem. Phys., 3,
446   181-193, doi 10.5194/acp-3-181-2003, 2003.

447   Ji, Y., Zhao, J., Terazono, H., Misawa, K., Levitt, N. P., Li, Y., Lin, Y., Peng, J., Wang, Y., Duan, L., Pan, B., Zhang, F., Feng,
448   X., An, T., Marrero-Ortiz, W., Secrest, J., Zhang, A. L., Shibuya, K., Molina, M. J., and Zhang, R.: Reassessing the
449   atmospheric oxidation mechanism of toluene, Proc. Natl. Acad. Sci. USA, 114, 8169-8174, 10.1073/pnas.1705463114, 2017.

450   Kahnt, A., Behrouzi, S., Vermeylen, R., Safi Shalamzari, M., Vercauteren, J., Roekens, E., Claeys, M., and Maenhaut, W.:
451   One-year study of nitro-organic compounds and their relation to wood burning in PM$_{10}$ aerosol from a rural site in Belgium,
452   Atmos. Environ., 81, 561-568, 10.1016/j.atmosenv.2013.09.041, 2013.

453   Kitanovski, Z., Grgic, I., Vermeylen, R., Claeys, M., and Maenhaut, W.: Liquid chromatography tandem mass spectrometry
454   method for characterization of monoaromatic nitro-compounds in atmospheric particulate matter, J. Chromatogr., A, 1268,
455   35-43, 10.1016/j.chroma.2012.10.021, 2012.

456   Laskin, A., Smith, J. S., and Laskin, J.: Molecular characterization of nitrogen-containing organic compounds in biomass

457   burning aerosols using high-resolution mass spectrometry, Environ. Sci. Technol., 43, 3764-3771, 10.1021/es803456n, 2009.

458   Lin, P., Bluvshtein, N., Rudich, Y., Nizkorodov, S. A., Laskin, J., and Laskin, A.: Molecular chemistry of atmospheric brown

459   carbon inferred from a nationwide biomass burning event, Environ. Sci. Technol., 51, 11561-11570, 10.1021/acs.est.7b02276,

460   2017.

461   Mohr, C., Lopez-Hilfiker, F. D., Zotter, P., Prevot, A. S., Xu, L., Ng, N. L., Herndon, S. C., Williams, L. R., Franklin, J. P.,

462   Zahniser, M. S., Worsnop, D. R., Knighton, W. B., Aiken, A. C., Gorkowski, K. J., Dubey, M. K., Allan, J. D., and Thornton,

463   J. A.: Contribution of nitrated phenols to wood burning brown carbon light absorption in Detling, United Kingdom during

464   winter time, Environ. Sci. Technol., 47, 6316-6324, 10.1021/es400683v, 2013.

465   Ng, N. L., Brown, S. S., Archibald, A. T., Atlas, E., Cohen, R. C., Crowley, J. N., Day, D. A., Donahue, N. M., Fry, J. L.,

466   Fuchs, H., Griffin, R. J., Guzman, M. I., Herrmann, H., Hodzic, A., Iinuma, Y., Jimenez, J. L., Kiendler-Scharr, A., Lee, B.

467   H., Luecken, D. J., Mao, J., McLaren, R., Mutzel, A., Osthoff, H. D., Ouyang, B., Picquet-Varrault, B., Platt, U., Pye, H. O.

468   T., Rudich, Y., Schwantes, R. H., Shiraiwa, M., Stutz, J., Thornton, J. A., Tilgner, A., Williams, B. J., and Zaveri, R. A.:

469   Nitrate radicals and biogenic volatile organic compounds: oxidation, mechanisms, and organic aerosol, Atmos. Chem. Phys.,

470   17, 2103-2162, 10.5194/acp-17-2103-2017, 2017.

471   Olariu, R. I., Klotz, B., Barnes, I., Becker, K. H., and Mocanu, R.: FT-IR study of the ring-retaining products from the

472   reaction of OH radicals with phenol, o-, m- and p-cresol, Atmos. Environ., 36, 3685-3697, 10.1016/S1352-2310(02)00202-9,

473   2002.

474   Purohit, V. and Basu, A. K.: Mutagenicity of nitroaromatic compounds, Chem. Res. Toxicol., 13, 673-692,

475   10.1021/tx000002x, 2000.

476   Renbaum-Wolff, L., Grayson, J. W., Bateman, A. P., Kuwata, M., Sellier, M., Murray, B. J., Shilling, J. E., Martin, S. T., and

477   Bertram, A. K.: Viscosity of α-pinene secondary organic material and implications for particle growth and reactivity, Proc.

478   Natl. Acad. Sci. USA, 110, 8014-8019, 10.1073/pnas.1219548110, 2013.

479   Sato, K., Hatakeyama, S., and Imamura, T.: Secondary organic aerosol formation during the photooxidation of toluene: NO_x

480   dependence of chemical composition, J. Phys. Chem. A, 111, 9796-9808, 10.1021/jp071419f, 2007.

481   Shrestha, M., Zhang, Y., Upshur, M. A., Liu, P., Blair, S. L., Wang, H. F., Nizkorodov, S. A., Thomson, R. J., Martin, S. T.,

482   and Geiger, F. M.: On surface order and disorder of alpha-pinene-derived secondary organic material, J. Phys. Chem. A, 119,

483   4609-4617, 10.1021/jp510780e, 2015.

484   Tang, R., Wu, Z., Li, X., Wang, Y., Shang, D., Xiao, Y., Li, M., Zeng, L., Wu, Z., Hallquist, M., Hu, M., and Guo, S.: Primary

485   and secondary organic aerosols in summer 2016 in Beijing, Atmos. Chem. Phys., 18, 4055-4068, 10.5194/acp-18-4055-2018,

486   2018.

487   Teich, M., van Pinxteren, D., Wang, M., Kecorius, S., Wang, Z., Müller, T., Močnik, G., and Herrmann, H.: Contributions of

488   nitrated aromatic compounds to the light absorption of water-soluble and particulate brown carbon in different atmospheric

489   environments in Germany and China, Atmos. Chem. Phys., 17, 1653-1672, 10.5194/acp-17-1653-2017, 2017.

490   Tham, Y. J., Wang, Z., Li, Q., Yun, H., Wang, W., Wang, X., Xue, L., Lu, K., Ma, N., Bohn, B., Li, X., Kecorius, S., Größ, J.,

491   Shao, M., Wiedensohler, A., Zhang, Y., and Wang, T.: Significant concentrations of nitryl chloride sustained in the morning:

492   investigations of the causes and impacts on ozone production in a polluted region of northern China, Atmos. Chem. Phys., 16,

493   14959-14977, 10.5194/acp-16-14959-2016, 2016.

494   Turpin, B. J. and Lim, H. J.: Species contributions to $PM_{2.5}$ mass concentrations: revisiting common assumptions for

495   estimating organic mass, Aerosol Sci. Tech., 35, 602-610, doi 10.1080/02786820152051454, 2001.

496   Vaden, T. D., Imre, D., Beranek, J., Shrivastava, M., and Zelenyuk, A.: Evaporation kinetics and phase of laboratory and

497   ambient secondary organic aerosol, Proc. Natl. Acad. Sci. USA, 108, 2190-2195, 10.1073/pnas.1013391108, 2011.

498   Vidovic, K., Lasic Jurkovic, D., Sala, M., Kroflic, A., and Grgic, I.: Nighttime aqueous-phase formation of nitrocatechols in

499   the atmospheric condensed phase, Environ. Sci. Technol., 52, 9722-9730, 10.1021/acs.est.8b01161, 2018.

500   Vione, D., Maurino, V., Minero, C., and Pelizzetti, E.: Phenol photonitration upon UV irradiation of nitrite in aqueous

501   solution I: effects of oxygen and 2-propanol, Chemosphere, 45, 893-902, 10.1016/s0045-6535(01)00035-2, 2001.

502   Vione, D., Maurino, V., Minero, C., Lucchiari, M., and Pelizzetti, E.: Nitration and hydroxylation of benzene in the presence

503   of nitrite/nitrous acid in aqueous solution, Chemosphere, 56, 1049-1059, 10.1016/j.chemosphere.2004.05.027, 2004.

504 Wang, H. C., Lu, K. D., Guo, S., Wu, Z. J., Shang, D. J., Tan, Z. F., Wang, Y. J., Le Breton, M., Lou, S. R., Tang, M. J., Wu,
505 Y. S., Zhu, W. F., Zheng, J., Zeng, L. M., Hallquist, M., Hu, M., and Zhang, Y. H.: Efficient N_2O_5 uptake and NO_3 oxidation
506 in the outflow of urban Beijing, Atmos. Chem. Phys., 18, 9705-9721, 10.5194/acp-18-9705-2018, 2018a.

507 Wang, L., Wang, X., Gu, R., Wang, H., Yao, L., Wen, L., Zhu, F., Wang, W., Xue, L., Yang, L., Lu, K., Chen, J., Wang, T.,
508 Zhang, Y., and Wang, W.: Observations of fine particulate nitrated phenols in four sites in northern China: concentrations,
509 source apportionment, and secondary formation, Atmos. Chem. Phys., 18, 4349-4359, 10.5194/acp-18-4349-2018, 2018b.

510 Wang, X., Gu, R., Wang, L., Xu, W., Zhang, Y., Chen, B., Li, W., Xue, L., Chen, J., and Wang, W.: Emissions of fine
511 particulate nitrated phenols from the burning of five common types of biomass, Environ. Pollut., 230, 405-412,
512 10.1016/j.envpol.2017.06.072, 2017a.

513 Wang, Y., Hu, M., Lin, P., Guo, Q., Wu, Z., Li, M., Zeng, L., Song, Y., Zeng, L., Wu, Y., Guo, S., Huang, X., and He, L.:
514 Molecular characterization of nitrogen-containing organic compounds in humic-like substances emitted from straw residue
515 burning, Environ. Sci. Technol., 51, 5951-5961, 10.1021/acs.est.7b00248, 2017b.

516 Wang, Y., Hu, M., Guo, S., Wang, Y., Zheng, J., Yang, Y., Zhu, W., Tang, R., Li, X., Liu, Y., Le Breton, M., Du, Z., Shang, D.,
517 Wu, Y., Wu, Z., Song, Y., Lou, S., Hallquist, M., and Yu, J.: The secondary formation of organosulfates under interactions
518 between biogenic emissions and anthropogenic pollutants in summer in Beijing, Atmos. Chem. Phys., 18, 10693-10713,
519 10.5194/acp-18-10693-2018, 2018c.

520 Weber, R. J., Guo, H., Russell, A. G., and Nenes, A.: High aerosol acidity despite declining atmospheric sulfate
521 concentrations over the past 15 years, Nature Geosci., 9, 282-285, 10.1038/ngeo2665, 2016.

522 Xie, M., Chen, X., Hays, M. D., Lewandowski, M., Offenberg, J., Kleindienst, T. E., and Holder, A. L.: Light absorption of
523 secondary organic aerosol: composition and contribution of nitroaromatic compounds, Environ. Sci. Technol., 51,
524 11607-11616, 10.1021/acs.est.7b03263, 2017.

525 Yuan, B., Liggio, J., Wentzell, J., Li, S.-M., Stark, H., Roberts, J. M., Gilman, J., Lerner, B., Warneke, C., Li, R., Leithead, A.,
526 Osthoff, H. D., Wild, R., Brown, S. S., and de Gouw, J. A.: Secondary formation of nitrated phenols: insights from
527 observations during the Uintah Basin Winter Ozone Study (UBWOS) 2014, Atmos. Chem. Phys., 16, 2139-2153,
528 10.5194/acp-16-2139-2016, 2016.

529 Yue, D., Hu, M., Wu, Z., Wang, Z., Guo, S., Wehner, B., Nowak, A., Achtert, P., Wiedensohler, A., Jung, J., Kim, Y. J., and
530 Liu, S.: Characteristics of aerosol size distributions and new particle formation in the summer in Beijing, J. Geophys. Res.,
531 114, D00G12, 10.1029/2008jd010894, 2009.

532 Zhang, X., Lin, Y. H., Surratt, J. D., and Weber, R. J.: Sources, composition and absorption Angstrom exponent of
533 light-absorbing organic components in aerosol extracts from the Los Angeles Basin, Environ. Sci. Technol., 47, 3685-3693,
534 10.1021/es305047b, 2013.

535 Zhang, Y., Sanchez, M. S., Douet, C., Wang, Y., Bateman, A. P., Gong, Z., Kuwata, M., Renbaum-Wolff, L., Sato, B. B., Liu,
536 P. F., Bertram, A. K., Geiger, F. M., and Martin, S. T.: Changing shapes and implied viscosities of suspended submicron
537 particles, Atmos. Chem. Phys., 15, 7819-7829, 10.5194/acp-15-7819-2015, 2015.

538 Zhang, Y. Y., Müller, L., Winterhalter, R., Moortgat, G. K., Hoffmann, T., and Pöschl, U.: Seasonal cycle and temperature
539 dependence of pinene oxidation products, dicarboxylic acids and nitrophenols in fine and coarse air particulate matter, Atmos.
540 Chem. Phys., 10, 7859-7873, 10.5194/acp-10-7859-2010, 2010.

541 Zhao, W., Fan, S., Guo, H., Gao, B., Sun, J., and Chen, L.: Assessing the impact of local meteorological variables on surface
542 ozone in Hong Kong during 2000–2015 using quantile and multiple line regression models, Atmos. Environ., 144, 182-193,
543 10.1016/j.atmosenv.2016.08.077, 2016.

544 Zheng, J., Hu, M., Du, Z. F., Shang, D. J., Gong, Z. H., Qin, Y. H., Fang, J. Y., Gu, F. T., Li, M. R., Peng, J. F., Li, J., Zhang,
545 Y. Q., Huang, X. F., He, L. Y., Wu, Y. S., and Guo, S.: Influence of biomass burning from South Asia at a high-altitude
546 mountain receptor site in China, Atmos. Chem. Phys., 17, 6853-6864, 10.5194/acp-17-6853-2017, 2017.

547

548

549

550

Figures

552

553
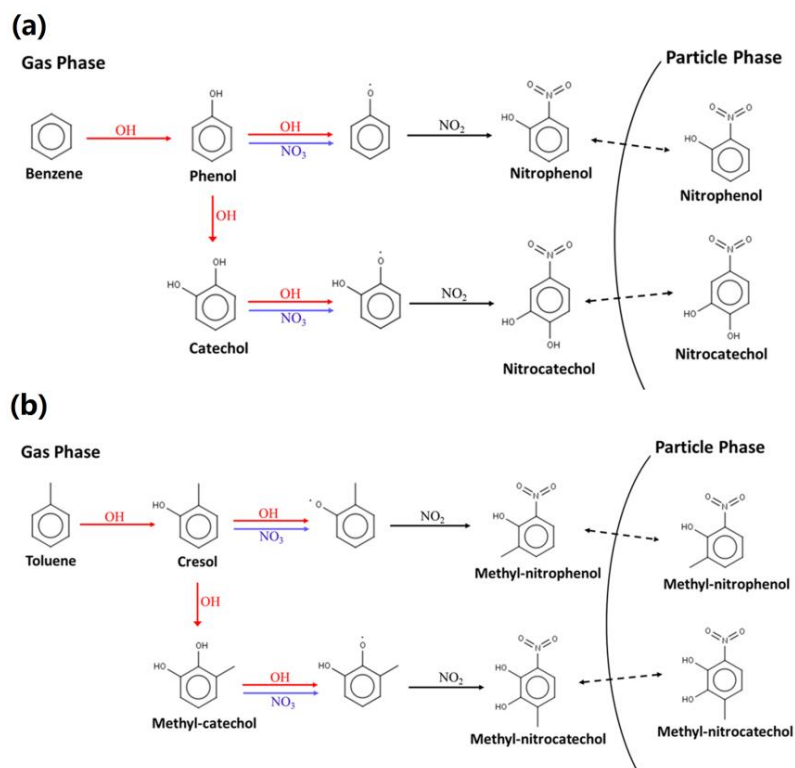
Figure 1 Formation of nitrophenols, nitrocatechols, methyl-nitrophenols and methyl-nitrocatechols from the oxidation of (a)

benzene and (b) toluene in the atmosphere (MCM v3.3). Reactions in red represent the daytime pathways and those in blue

represent the nighttime pathways. Other isomers for intermediate and final products are also expected, but not shown in the

figure for clarity.

558
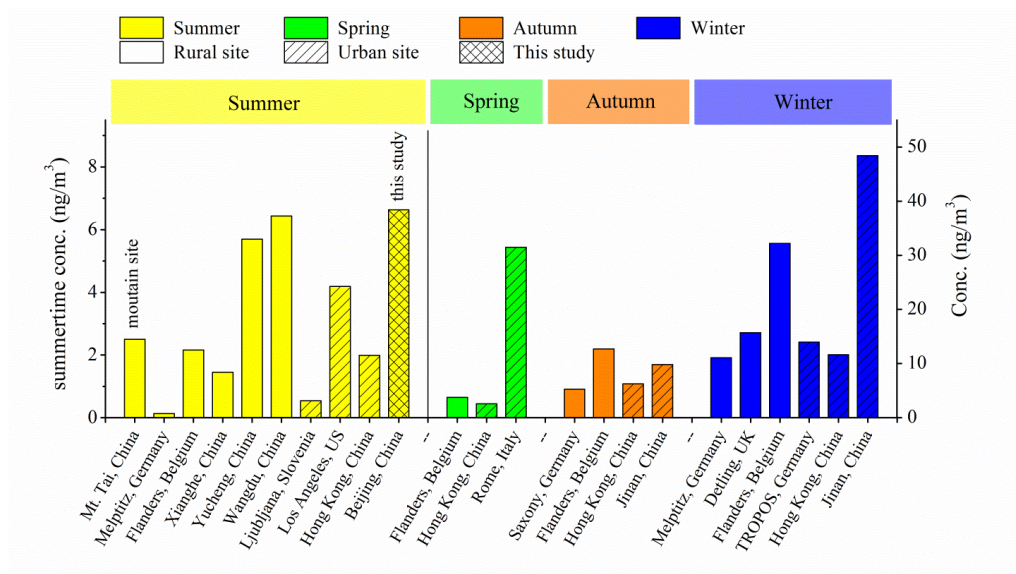
559

560 Figure 2 Summary of NAC concentrations cross this and prior studies (see Table S1 for the data and references therein). The

561 NAC concentrations in summer correspond to the left axis and other seasons correspond to the right axis.

562
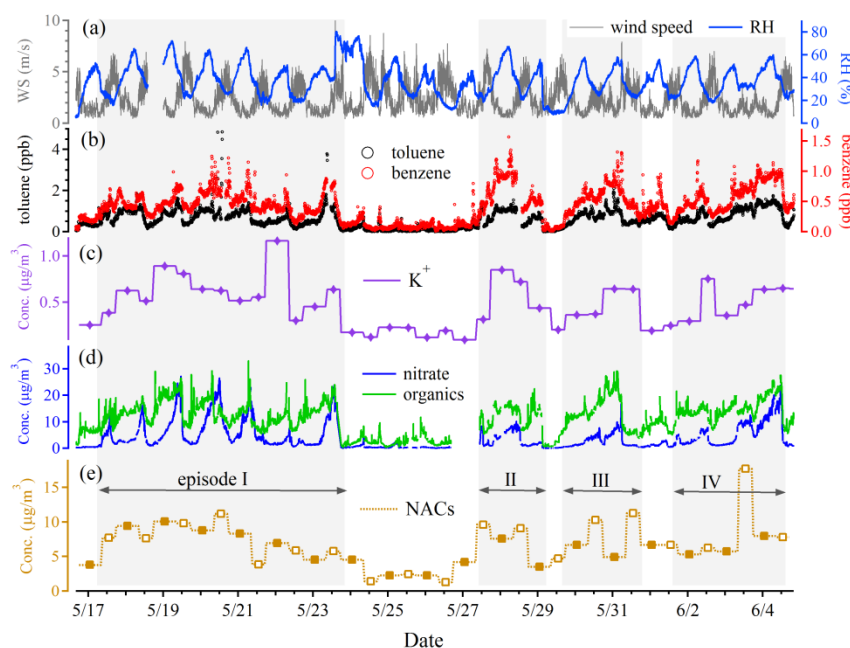
563

564 Figure 3 Time series of (a) wind speed (WS) and relative humidity (RH), (b) benzene and toluene, mass concentrations of (c)

565 K^+, (d) organics and nitrate, and (e) NACs. The pollution episodes are marked by gray shading.

566
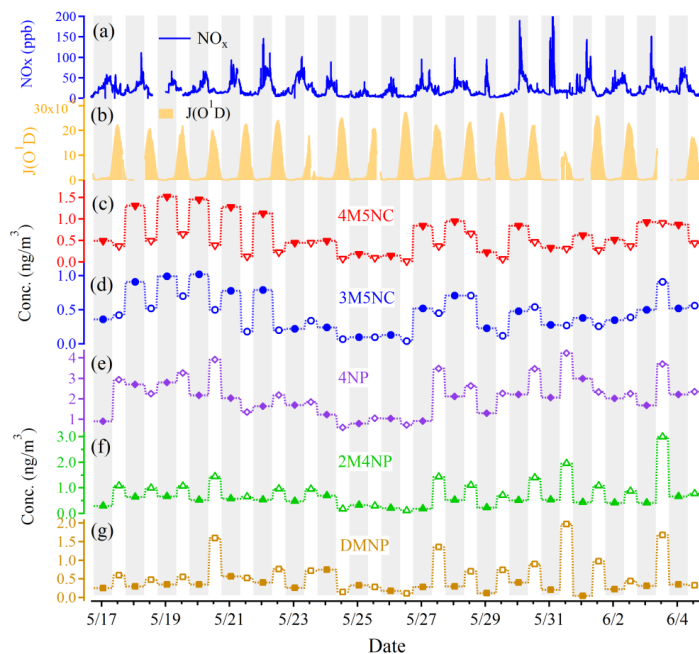
567

568   Figure 4 Time series of (a) NO$_x$, (b) J(O^{1}D), (c) 4-methyl-5-nitrocatechol (4M5NC), (d) 4-methyl-5-nitrocatechol (3M5NC),

569   (e) 4-nitrophenol (4NP), (f) 2-methyl-4-nitrophenol (2M4NP), and (g) dimethyl-nitrophenol (DMNP). The gray background

570   denotes the nighttime and white background denotes the daytime.

571
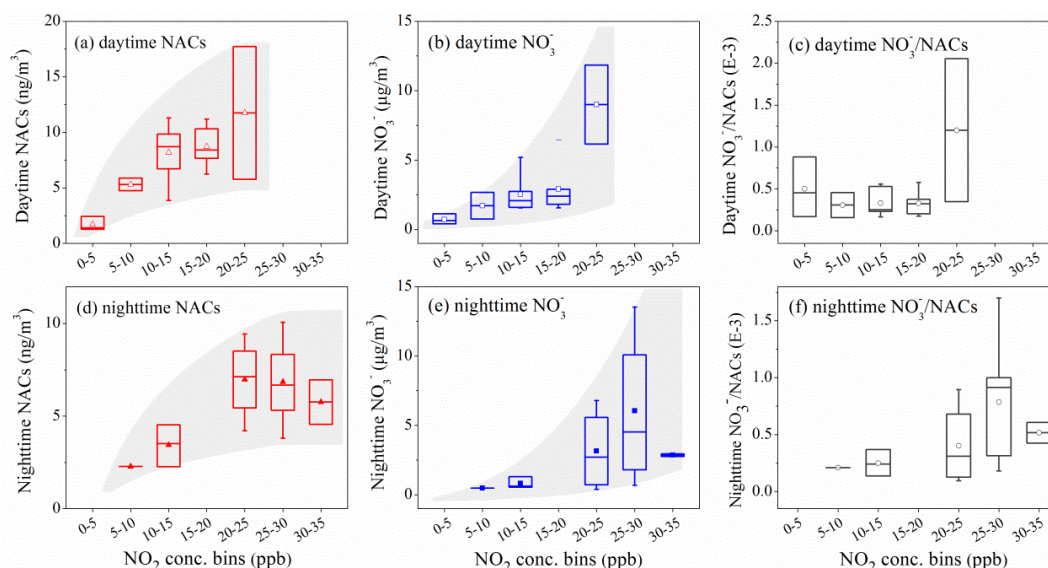
572

573   Figure 5 Concentrations of NACs, nitrate and NO$_3^-$/NAC ratios as a function of NO$_2$ concentration bins during daytime and

574   nighttime. The markers represent the mean values and whiskers represent 25 and 75 percentiles.

575
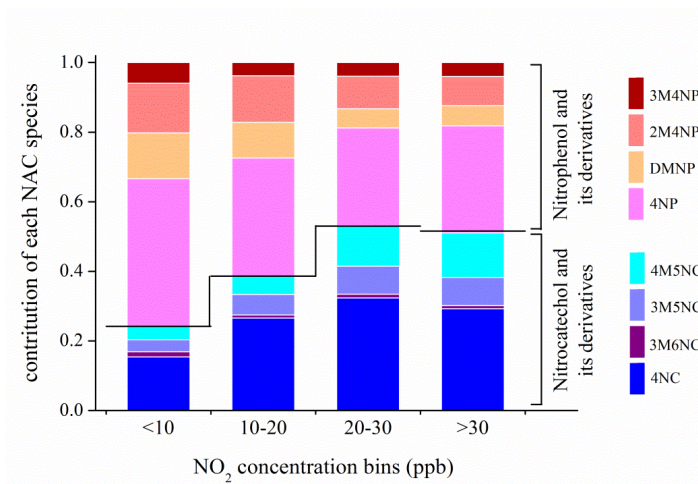
576

577 Figure 6 Variation of NAC compositions as a function of NO$_2$ concentration bins.

578
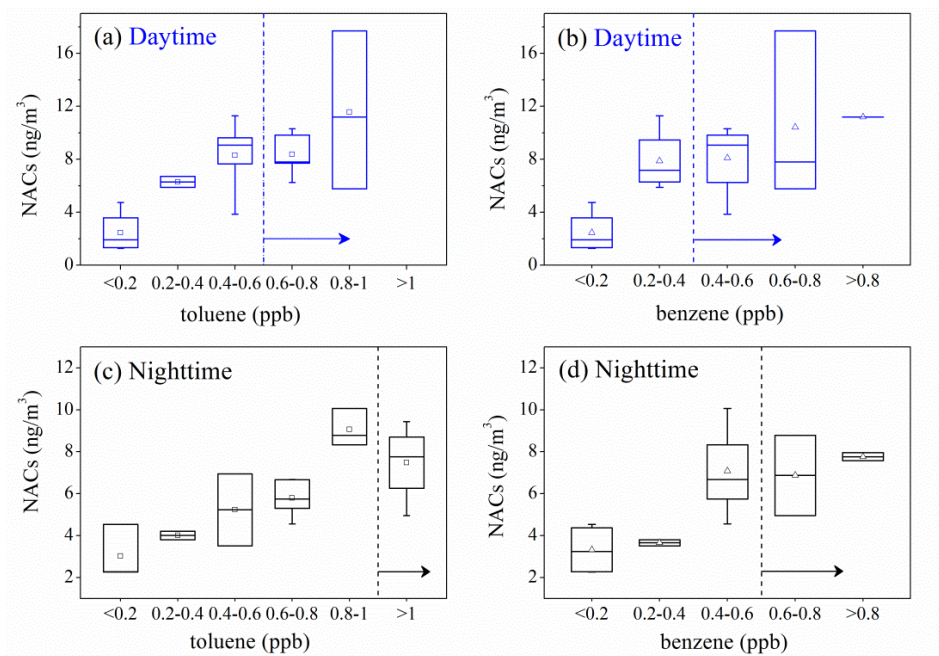
579

580 Figure 7 Concentrations of NACs as a function of toluene and benzene concentration bins during daytime and nighttime. The

581 markers represent the mean values and whiskers represent 25 and 75 percentiles. The r value in each panel represents the

582 correlation coefficient between NACs and toluene or benzene.

583

584
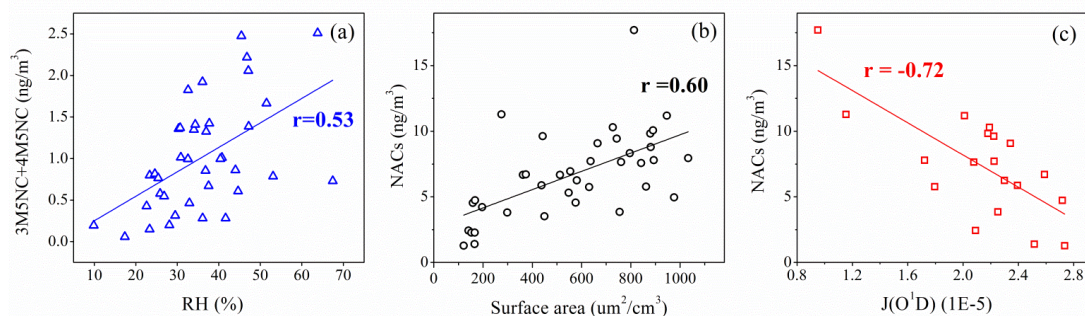
585

586   Figure 8 Correlation analysis (a) between (3M5NC+4M5NC) and RH, (b) between NACs and aerosol surface area, (c)

587   between NACs and J(O^{1}D).

588
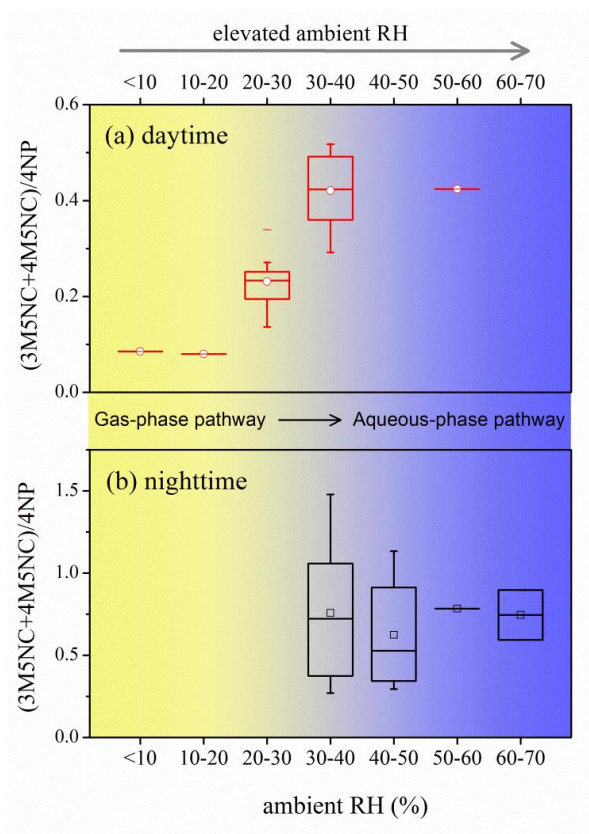
589

590   Figure 9 (3M5NC+4M5NC)/4NP concentration ratios as a function of ambient RH during (a) daytime and (b)

591   nighttime.

592

593

594

595 **Tables**

596 Table 1 Quantified nitro-aromatic compounds in this study

compounds	formula	[M-H]⁻	retention time (min)	standard	structure	range	average (n=38)
4NP	$C_6H_4NO_3^-$	138.02	21.3	4NP		0.60-4.24	2.15±0.93
3M4NP	$C_7H_6NO_3^-$	152.03	23.9	3M4NP		0.08-0.64	0.27±0.12
2M4NP	$C_7H_6NO_3^-$	152.03	24.9	2M4NP		0.11-2.99	0.76±0.55
DMNP	$C_8H_8NO_3^-$	166.05	26.0, 26.3, 26.9	2,6DM4NP		0.04-1.97	0.55±0.45
Total NP							3.72
4NC	$C_6H_4NO_4^-$	154.01	18.9	4NC		0.16-6.89	1.89±1.28
4M5NC	$C_7H_6NO_4^-$	168.03	21.8	4M5NC		0.02-1.52	0.56±0.40
3M6NC	$C_7H_6NO_4^-$	168.03	23.2	4M5NC		0.02-0.19	0.07±0.03
3M5NC	$C_7H_6NO_4^-$	168.03	23.5	4M5NC		0.04-1.02	0.44±0.27
Total NC							2.96

597